INSTITUTE OF PHYSICS PUBLISHING JOURNAL OF PHYSICS B: ATOMIC, MOLECULAR AND OPTICAL PHYSICS

J. Phys. B: At. Mol. Opt. Phys. **37** (2004) 1113–1124 PII: S0953-4075(04)73083-7

Superelastic electron scattering from laser excited rubidium at 20 eV incident energy

B V Hall[1,3], Y Shen[1], A J Murray[1,4], M C Standage[1], W R MacGillivray[1,5] and I Bray[2]

[1] Laser Atomic Physics Laboratory, School of Science, Griffith University, Nathan 4111, Australia
[2] School of Mathematical and Physical Sciences, Murdoch University, Murdoch 6150, Australia

Received 3 December 2003
Published 23 February 2004
Online at stacks.iop.org/JPhysB/37/1113 (DOI: 10.1088/0953-4075/37/5/014)

Abstract

Superelastic electron scattering measurements are presented from rubidium atoms excited by laser radiation to the 5^2P states at around 780 nm. The incident energy of the electrons was 18.4 eV corresponding to 20 eV incident electrons for the excitation process 5^2S–5^2P. The measurements were conducted over a range of scattering angles from 5° through to 125°. A complete set of atomic collision parameters for the interaction process is presented together with the associated pseudo-Stokes parameters obtained from the measurements. A comparison with three sophisticated theoretical models indicates that none of the models completely describes the interaction process at this energy, and that further experimental and theoretical work is needed.

1. Introduction

Measurement of atomic collision parameters (ACPs) for electron collisions with atoms has enabled more stringent tests of modern theoretical models than differential cross section data. ACPs, sometimes referred to as electron impact coherence parameters (EICPs), enable the determination of both amplitudes and relative phases of the scattering matrix elements that describe the collision process (Andersen *et al* 1988).

An experimental technique that has been employed with considerable success is the electron superelastic scattering method (Hertel and Stoll 1974, Registar *et al* 1978, Farrell *et al* 1989, Scholten *et al* 1993, Li and Zetner 1994, Law and Teubner 1995, Karaganov *et al* 1996, Stockman *et al* 1998). In these experiments, electrons are scattered from excited atomic states, which have been prepared by resonant interaction with laser radiation. Those electrons that gain energy by de-exciting the atom are detected and analysed as a function of the laser

[3] Present address: Imperial College, London, UK.
[4] Present address: AMLaM Group, Schuster Laboratory, University of Manchester, Manchester M13 9PL, UK.
[5] Present address: Faculty of Sciences, University of Southern Queensland, Toowoomba 4350, Australia.

polarization. By invoking time-reversal invariance arguments, atomic collision parameters for the electron excitation of the atomic state can be deduced from this superelastic scattering process.

The first atomic target studied by this method was sodium. ACPs for excitation of the 3S–3P transition have been reported by a number of groups for a range of incident electron energies (Hertel and Stoll 1974, Farrell *et al* 1989, Scholten *et al* 1993, Sang *et al* 1994). In general, very good agreement between the measured data and calculated parameters using various models of scattering theory has been achieved. In particular, the convergent close-coupling model (CCC) (Bray 1994) has been successful in closely reproducing experimental results.

The alkali atoms are very attractive candidates for studies of electron–atom collisions using the superelastic scattering method since the ground S-state to first excited P-state transition is usually readily accessed by continuous wave, single-mode laser radiation. Further, the line strength of these transitions enables efficient excitation of atoms to the P-state. Subsequent to the studies on sodium, the Flinders group has published data for lithium and potassium (Karaganov *et al* 1996, Stockman *et al* 1998). Excellent agreement with CCC calculations was again achieved.

All of the above studies were undertaken under conditions in which *LS* coupling holds. Under these conditions, the relativistic contribution to the interaction potential is small and the incidence of spin-flip of the target valence electron is negligible. This paper reports on the first study of electron superelastic scattering from rubidium. As rubidium is a heavier element than sodium, it is more likely that *LS* coupling may break down during the collision between electrons and rubidium atoms, and so the ACP data obtained is for a regime that further tests the effectiveness of the different theoretical models.

The ACPs which provide the best physical insight into the excitation collision process are those associated with the natural frame, in which the quantization axis (z-axis) is perpendicular to the scattering plane, defined as that containing the incident ($\mathbf{k_i}$) and scattered ($\mathbf{k_f}$) electrons. The direction of the z-axis is then defined by $\mathbf{k_i} \times \mathbf{k_f}$. Four ACPs are defined for excitation by unpolarized electrons. These are the alignment parameters $P^+_{\rm lin}$ and γ^+, the orientation parameter $L^+_\perp$ and the spin-flip parameter ρ_{00}. $P^+_{\rm lin}$ describes the relative shape of the excited P-state charge cloud and γ^+ is the angle between the major axis of the charge cloud and $\mathbf{k_i}$. $L^+_\perp$ represents the transfer of angular momentum in the z-direction during the collision. The final parameter ρ_{00} is a measure of the 'height' of the charge cloud at the origin. When ρ_{00} is non-zero, this signifies the breakdown of *LS* coupling and the presence of significant relativistic interaction. The ACPs are defined using the notation of Andersen *et al* (1988) where the superscript, '+', represents a parameter with positive reflection symmetry through the scattering plane. A schematic of the charge cloud in the scattering plane for the time inverse superelastic scattering method is shown in figure 1.

To obtain values for the four ACPs, four independent measurements are required in the experiment. Three measurements are conducted with the laser radiation propagating in the opposite direction to the natural frame quantization axis (figure 1). The differential cross sections for superelastic scattering of electrons are then measured as a function of the laser polarization. Pseudo-Stokes parameters are calculated from these measurements (Farrell *et al* 1991),

$$P_1^S = (S_0(\theta) - S_{90}(\theta))/(S_0(\theta) + S_{90}(\theta)) \tag{1a}$$

$$P_2^S = (S_{45}(\theta) - S_{135}(\theta))/(S_{45}(\theta) + S_{135}(\theta)) \tag{1b}$$

$$P_3^S = (S_{\rm RHC}(\theta) - S_{\rm LHC}(\theta))/(S_{\rm RHC}(\theta) + S_{\rm LHC}(\theta)) \tag{1c}$$

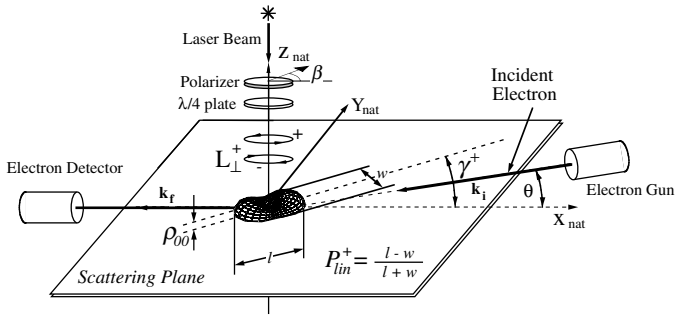

Figure 1. Schematic of the P-state charge cloud in the scattering plane for the superelastic scattering method. The natural frame atomic collision parameters are shown, together with the direction of the laser beam orthogonal to the scattering plane.

where the terms S_β represent the differential cross section with the laser light linearly polarized at angle β to the natural frame x-axis (figure 1) or, in the case of circularly polarized light, represent right- or left-hand circular polarization.

The fourth measurement which is required to completely determine all four ACPs is made by injecting linearly polarized laser radiation in the scattering plane along the x-axis. The ratio, r, of the electron superelastic differential cross section for polarization parallel and perpendicular to the scattering plane (Hermann *et al* 1977) is then measured,

$$r = S_\parallel / S_\perp. \tag{2}$$

Using the principle of micro-reversibility, the pseudo-Stokes parameters can be related to the normal Stokes parameters, P_i, defined for electron impact excitation of the transition (Farrell *et al* 1991) using the following transformations:

$$P_1^S = \frac{(1-\rho_{00})K P_1}{(1-K\rho_{00})} \tag{3a}$$

$$P_2^S = \frac{(1-\rho_{00})K P_2}{(1-K\rho_{00})} \tag{3b}$$

$$P_3^S = \frac{(1-\rho_{00})K' P_3}{(1-\rho_{00}) + K''\rho_{00}} \tag{3c}$$

$$r = \frac{1 - K\rho_{00} - (1-\rho_{00})K P_1}{1 - K + 2K\rho_{00}} \tag{3d}$$

where K, K' and K'' are parameters that describe the optical preparation of the excited atomic state. All three optical pumping parameters have been defined using a sophisticated QED model in previous work (Farrell *et al* 1991, Hall 1998). For the ground S-state to P-state transition in an alkali atom, K is identical to the line polarization, $P_L = (I_0 - I_{90})/(I_0 + I_{90})$ for the resonance fluorescence spontaneously emitted by the P-state along the natural frame y-axis following excitation by linearly polarized laser radiation incident along the negative z-axis with field vector parallel to the x-axis. I_β represents the fluorescence intensity analysed by a linear polarizer whose axis is at an angle β to the x-axis. In the superelastic scattering experiments reported here, the laser is tuned to the $5^2S_{1/2}(F=3) - 5^2P_{3/2}(F=4)$ hyperfine transition for ^{85}Rb and to the $5^2S_{1/2}(F=2) - 5^2P_{3/2}(F=3)$ transition for ^{87}Rb. K is measured as $K = 0.40 \pm 0.01$ and $K = 0.43 \pm 0.01$ for ^{85}Rb and ^{87}Rb respectively under the conditions used in these experiments.

The optical pumping parameter K' describes the optical pumping in the P-state manifold by circularly polarized radiation incident along the negative z-axis. This parameter is difficult to determine experimentally (Fischer and Hertel 1982) as it requires the measurement of the line polarization for fluorescence emitted in the propagation direction of the laser radiation. However, since the atoms spend many lifetimes within the laser beam, almost complete optical pumping can be achieved, resulting in K' having a magnitude very close to unity. Detailed quantum electrodynamic calculations for the conditions of the experiments reported here yield values of K' given by $K' = -0.985$ and $K' = -0.982$ respectively for the ^{85}Rb and ^{87}Rb isotopes (Hall *et al* 1999).

For S-state to P-state transitions, K'' is identical to the ratio I_{90}/I_0 of resonance fluorescence spontaneously emitted along the y-axis following excitation by circularly polarized laser radiation propagating along the negative z-axis. For the experimental conditions used in the superelastic scattering measurements reported here, K''values were determined to be $K'' = 0.10 \pm 0.01$ and $K'' = 0.08 \pm 0.01$ respectively for the ^{85}Rb and ^{87}Rb isotopes.

The ACPs may be determined from the Stokes parameters via (Andersen *et al* 1988),

$$P_{\text{lin}}^{+} = \sqrt{P_1^2 + P_2^2} \tag{4a}$$

$$L_{\perp}^{+} = -P_3 \tag{4b}$$

$$\gamma^{+} = \tfrac{1}{2}\arg(P_1 + \mathrm{i}P_2) \tag{4c}$$

with ρ_{00} determined directly from equations (3).

One further useful parameter is defined as the degree of polarization P_{tot} (Andersen *et al* 1988):

$$P_{\text{tot}} = \sqrt{P_1^2 + P_2^2 + P_3^2} = \sqrt{P_{\text{lin}}^{+2} + L_{\perp}^{+2}} \tag{5}$$

2. The experimental apparatus

The apparatus used in these experiments was an improved version of that used previously in superelastic scattering studies of Na and which was described in detail by Farrell *et al* (1989) and Sang *et al* (1994). A stainless steel vacuum chamber contained the components required for a cross beam experiment, namely an oven to produce the atomic beam, an unselected energy electron gun and an electron analyser. These items were mounted on concentric turntables inside the chamber, allowing the electron gun to rotate around the scattering plane independent of the analyser. A schematic of the components and their layout is given in figure 2. A continuous wave (CW) laser beam from a Coherent 899 Ti:Sapphire laser was injected into the interaction region perpendicular to the scattering plane for measurement of the P_j^S parameters and was injected in-plane through the electron analyser to determine ρ_{00}.

The oven used in these studies was a standard heated crucible type consisting of a reservoir of rubidium and a differentially heated nozzle. The oven produced a beam of Rb in its natural abundance (72% ^{85}Rb, 28% ^{87}Rb) with an estimated density of 10^{10} cm^{-3} in the interaction region. By recording the fluorescence spectrum from the atoms excited using very low laser power, a Doppler width of approximately 200 MHz was estimated. The electron detector, described in detail previously (Sang *et al* 1994) consisted of a cylindrical analyser and a channeltron. The vacuum chamber was internally lined with 2 mm thick μ-metal and was surrounded by three pairs of mutually orthogonal Helmholtz coils. The magnetic field in the interaction region was reduced to below 0.01 μT by adjustment of the current in the coils.

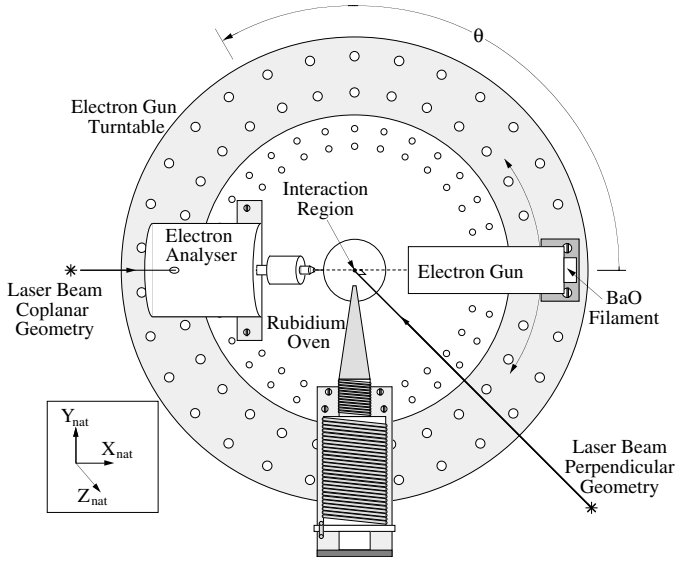

Figure 2. Schematic of the apparatus components inside the scattering chamber. The oven and electron analyser are located on the inner (stationary) turntable while the electron gun rotates with the outer turntable. The laser beam enters the chamber orthogonal to the scattering plane, or through the analyser as shown.

Several improvements to the apparatus which has been described previously (Farrell *et al* 1989) were made for these new experiments. A new electron gun was constructed, using a design identical to that used in the (e, 2e) experiment at Manchester (Murray *et al* 1992a, 1992b). The gun incorporated a BaO filament to improve the energy resolution while maintaining a beam current of several hundred nano-amps in the interaction region. The gun, in conjunction with the electron analyser, produced an energy resolution of around 300 meV at 18.4 eV electron energy with a beam angle of zero degrees and a pencil angle of 2°. The energy resolution provided by the BaO filament was required in these experiments since the excitation energy of the P-state is only 1.6 eV, and it was necessary to resolve the superelastic signal from the elastic peak. The energy of the electron gun was calibrated by looking for the onset of excitation of the 2^3S_1 and 2^1S_0 metastable states of helium, which occur at energies of 19.82 eV and 20.62 eV respectively.

The frequency drift of the laser was stabilized for long periods of time by locking the laser control electronics to the saturated absorption signal derived from Rb in an external vapour cell. Details of the control electronics and stabilization technique have been published elsewhere (Varcoe *et al* 2000). Although measurements of individual pseudo-Stokes parameters at any given scattering angle only took a few minutes, stabilization of the laser frequency enabled repeated measurements to be conducted over a long period of time with the confidence that the laser tuning conditions remained unchanged throughout the measurements.

To align the analyser, electron gun, oven and laser beam to the interaction region, an alignment tool was constructed which incorporated collimated visible laser diodes operating at 650 nm to determine the axis of rotation of the turntables and to define the scattering plane (Hall 1998). This device enabled the atomic beam, exciting laser beam, electron gun and electron analyser to be accurately aligned to the rotation centre. Once the alignment procedure was completed, the electron gun could be rotated over the entire available angular range from +120° to −75°, while remaining aligned to the centre of rotation.

The final improvement to the system was in terms of the scattering angle calibration. Zero degrees was determined by replacing the grid assembly in the gun with a visible laser diode so that the laser beam accurately defined the gun axis. The gun was then rotated until the laser beam passed cleanly through the analyser defining apertures. This zero-angle position was registered by mounting a small plate on the gun's turntable to interrupt the signal between an infrared LED and a photo-transistor. Measurement of $L_{\perp}^{+}$, which passes through the origin, indicated that the electron scattering zero angle was offset by approximately -3° from geometric zero. This difference is probably due to differences in the mechanical and the electrostatic alignment of the system, which is influenced by the electron lens and deflectors in the electron gun and analyser. To compensate for this difference, all measurements were adjusted by this amount. It was estimated that each angle could be determined to within $\pm 1^{\circ}$. The acceptance angle of the cylindrical analyser input lens was $\pm 3^{\circ}$, and so the total angular resolution of the spectrometer was around $\pm 3.5^{\circ}$.

The experimental protocol adopted here was unchanged from that previously reported. With all components of the apparatus functioning correctly and at their appropriate settings, the electron gun was rotated to the required scattering angle. The desired polarization of the laser radiation was created by a combination of a Glan–Taylor linear polarizer and a zero order quarter wave plate, each housed in mounts which could be independently rotated by stepper motors. The stepper motors were controlled by a personal computer which was programmed to position the polarization optics to the correct relative positions for the pseudo-Stokes parameter or coplanar parameter being measured.

The electron analyser was adjusted to detect electrons that gained 1.6 eV from the collision. Hence the electrons that de-excited atoms from the $5^2P_{3/2}$ state by gaining the transition energy were detected by a channeltron and, following amplification and discrimination, the associated pulses were recorded using an ORTEC timer/counter. Superelastically scattered electrons were counted for a specific time period and then the polarizer was rotated to the next setting. A background count was taken at each polarizer setting by inserting a beam stop into the laser beam prior to the polarizers. The beam stop was operated by a relay which was switched under computer control.

Each pseudo-Stokes parameter was obtained by calculating the mean value from around 40 separate experimental measurements. To reduce systematic errors introduced by the stepper motors controlling the polarizer and quarter wave plates, 50% of these measurements were made at polarizer angles (θ_1, θ_2) and 50% at polarizer angles $(\theta_1 + \pi, \theta_2 + \pi)$, where θ_1 and θ_2 represent the polarizer angles required to define the pseudo-Stokes parameter being measured. The error bars on all reported data represent one statistical standard deviation. Measurements for both isotopes were made sequentially at each scattering angle by tuning the laser to the appropriate transition frequency. The gun was then rotated to the next angular position. A check of the symmetry conditions around the forward direction was made by rotating the gun to selected negative-scattering angles. The conditions

$$P_1^S(\theta) = P_1^S(-\theta) \qquad P_2^S(\theta) = -P_2^S(-\theta) \qquad P_3^S(\theta) = -P_3^S(-\theta) \tag{6}$$

were found to be satisfied within the statistical error.

Measurements for the complete scattering range from 0° to 120° could not be obtained from the apparatus geometry shown in figure 2. When the electron gun was approximately opposite the nozzle of the oven, elastic scattering of electrons from the nozzle swamped the superelastic signal. Degradation of the performance of the gun in this configuration was also observed over time as some rubidium was deposited on the lens elements. Measurement of the pseudo-Stokes parameters in the range 70° to 100° was therefore achieved by moving the

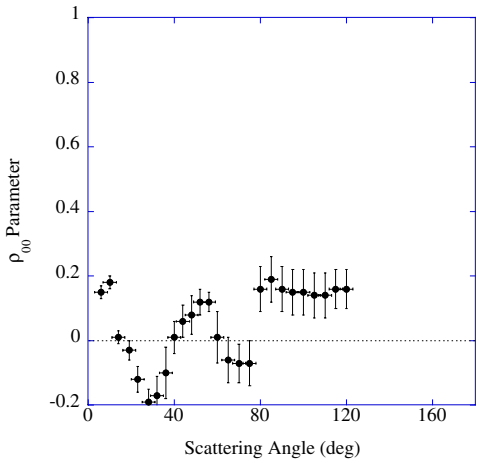

Figure 3. Measured values of ρ_{00}, seen to vary from +0.2 to −0.2. Measured values less than 0 are unphysical, and indicate the uncertainty in this parameter. For details, see text.

oven to a position close to the analyser, at an angle approximately 40° to the vertical (negative y-axis).

For the in-plane measurements, the low signal-to-noise ratios which were observed for the ^{87}Rb meant that statistically reliable data could only be obtained for scattering angles up to 45°. In contrast, data were obtained at scattering angles up to 120° for ^{85}Rb by repositioning the oven in the scattering plane. This introduced a Doppler shift in the atomic transition, which meant that the external locking electronics could not be used for these measurements, and the laser was kept on resonance by monitoring fluorescence.

3. Results

The measured data for ρ_{00} are presented in figure 3. No calculated values for this parameter are available. The measured values for this parameter range between $\rho_{00} = \pm 0.2$. By definition, ρ_{00} can only take on positive values, and so the negative values recorded here give an indication of the systematic error in this measurement. This uncertainty may be due to a number of different factors. Insertion of the laser beam exactly in the scattering plane defined by the incident and scattered electrons is technically difficult, whereas the effect on the definition of the plane at forward scattering angles on the measurement of ρ_{00} has been analysed in detail (Zetner *et al* 1990). The difficulty in defining the plane at low scattering angles is further increased when the laser beam must also be defined in this plane. Contributions to the measurements from a range of scattering planes, known as the finite volume effect, can lead to spurious and non-physical values of the measured ρ_{00} parameter for this geometry.

From these considerations we have tentatively concluded that ρ_{00} is approximately zero under these experimental conditions. This conclusion is informed not only by our measurements, but by calculations of the fine-structure resolved spin polarization function, S_P (Andersen *et al* 1997). If the atomic transition is well described by LS coupling, then the symmetry relationship $S_P(^2\mathrm{P}_{1/2}) \approx -2S_P(^2\mathrm{P}_{3/2})$ holds (Hanne 1983). The calculations predict that for direct excitation by 20 eV electrons (equivalent to superelastic de-excitation by 18.4 eV electrons), the fine structure relationship is satisfied until about 90° scattering. If

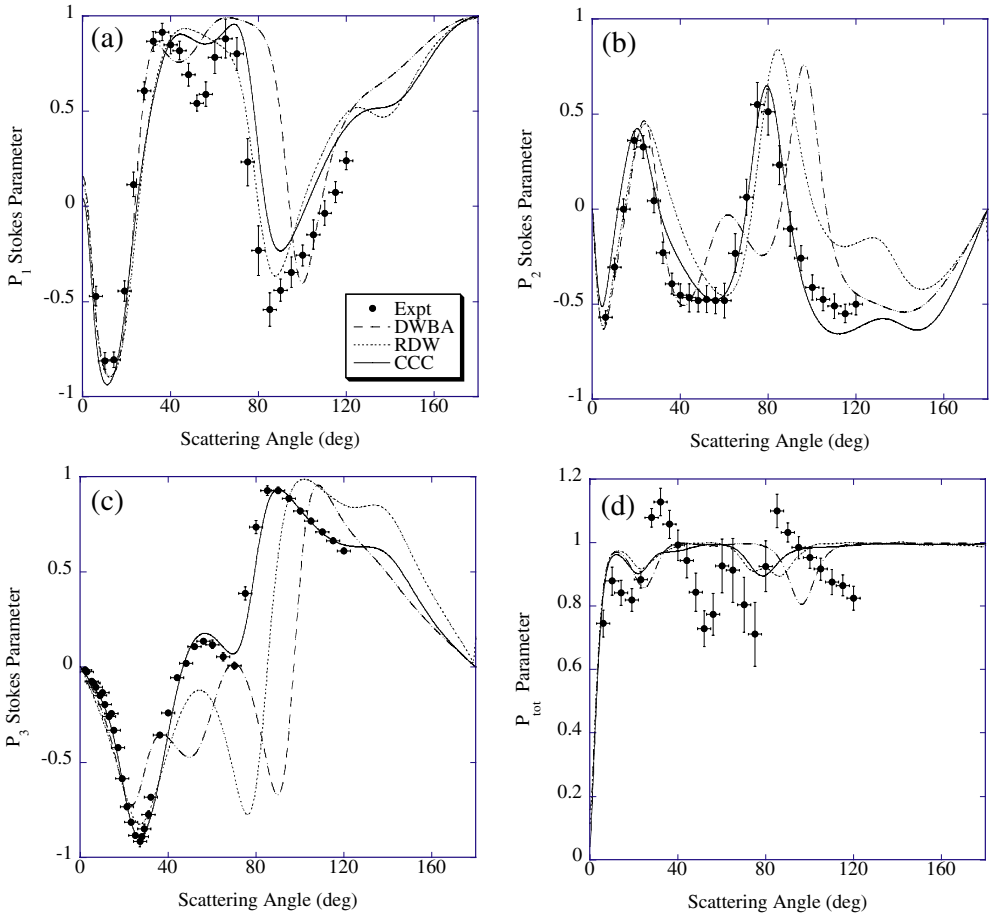

Figure 4. Measured values of the Stokes parameters P_1 (a), P_2 (b) and P_3 (c) together with the deduced total polarization $P_{\rm tot}$ (d). Also plotted are calculations from theory: CCC (solid line), DWBA (dashed line) and the RDW model (dotted line).

LS coupling holds, then ρ_{00} is expected to be zero up to this angle as there is no spin-flip of the incident electron.

The Stokes parameters, deduced from the measured pseudo-Stokes parameters using equations (3*a*) to (3*c*) are shown in figure 4, along with $P_{\rm tot}$. The measured data is a weighted average of measurements from the two isotopes, since no differences were seen between the results from each isotope within experimental uncertainty. The experimental data are compared with results from the present non-relativistic convergent close-coupling (CCC) and distorted-wave Born (DWBA) calculations, as well as the relativistic distorted-wave (RDW) calculations of Zeman *et al* (1998). All calculations have been convoluted with the estimated apparatus angular resolution.

The details of the CCC method for electron-alkali atom scattering have been given by Bray (1994). Briefly, the atom is treated as having one active valence electron above an inert Hartree–Fock core. In addition, virtual excitation of the core is treated via phenomenological one- and two-electron core-polarization potentials. These are particularly significant for the heavier alkalis and are used to ensure sufficiently accurate one-electron ionization energies and oscillator strengths.

These approximations define the target Hamiltonian which is then diagonalized using the orthogonal Laguerre basis with the exponential fall-off parameter $\lambda = 6$ to obtain the target states. In the present case we use $N_l = N_0 - l$ basis functions with $N_0 = 50$ and $l \leqslant 3$.

These functions generated a sufficient number of open negative- and positive-energy states for convergence in the parameters of interest. Only one closed state has been retained for each value of l leading to a total of 47 states with a maximum of 116 channels. The coupled equations were solved to obtain T-matrix elements for partial waves $L \leqslant 60$ with those for $L > 60$ being considered using analytical techniques. The T-matrix elements are used to define the 5s–5p scattering amplitude from which all physical observables may be defined. We also used the CCC computer code in the DWBA mode where exchange and channel-coupling are neglected. Whereas in the CCC calculation the distorting potential is used as a numerical aid, with the final result being independent of the choice of this potential, the DWBA results do depend on the choice. The DWBA presented here used the static ground state potential in both the initial and final channels.

For the RDW model the final static potential for the 5P-state was used for the distortion potential in both initial and final channels, the RDW model also utilising a relativistic formalism (Zeman *et al* 1998). In the non-relativistic formalism the two 5p levels ($5^2P_{1/2}$ and $5^2P_{3/2}$) in rubidium are not distinguishable. This non-relativistic fine structure approximation treats the electron–atom interaction using *LS*-coupling; as a consequence the spin polarization of the continuum electron can only change through electron exchange. When the incident electron penetrates deep into the rubidium atom, as for large angle scattering, relativistic effects like spin–orbit interactions may become significant. Under these conditions direct spin-flip due to spin–orbit interaction can occur and may dominate over spin-flip due to electron exchange. At this point the fine structure approximation fails and it is necessary to treat scattering to the individual fine structure states of the atom separately. The RDW formalism describes the electron–atom interaction using the *jj*-coupling scheme and uses the Dirac equation rather than the Schrödinger equation. The individual fine structure states of the atomic target are therefore calculated directly without the required re-coupling involved in the *LS* scheme. The Dirac equation also incorporates spin-dependent effects. The RDW model can therefore predict spin-flip due to spin–orbit coupling, a relativistic effect that increases with atomic number Z. Since the superelastic scattering technique is able to resolve the $2P_{3/2}$ fine structure level of rubidium, the RDW theory can calculate the required scattering amplitudes directly (Zeman *et al* 1998).

4. Discussion

The P_1 Stokes parameter results (figure 4(a)) are not reproduced accurately by any of the calculations, although each of the curves and the data have the same general shape. The data does not give insight into which of the models is the most accurate for this parameter. At forward scattering angles, the models agree with each other and moderately well with the data to 25°. Then to a scattering angle of 45°, the DWBA model is in closest agreement. The minimum observed in the data around 45° is not predicted by any of the models, although the CCC and DWBA models show a shallow minimum in this region. For the region between 65° and 85° where the value of the parameter rapidly decreases to a minimum, the RDW model does slightly better than the CCC model. The DWBA curve has its minimum approximately 15° higher in scattering angle. All models essentially overestimate this parameter at scattering angles beyond this minimum.

A similar situation is apparent for the P_2 Stokes parameter (figure 4(b)). The DWBA calculations yield the closest agreement with the data at small scattering angles to 45° while

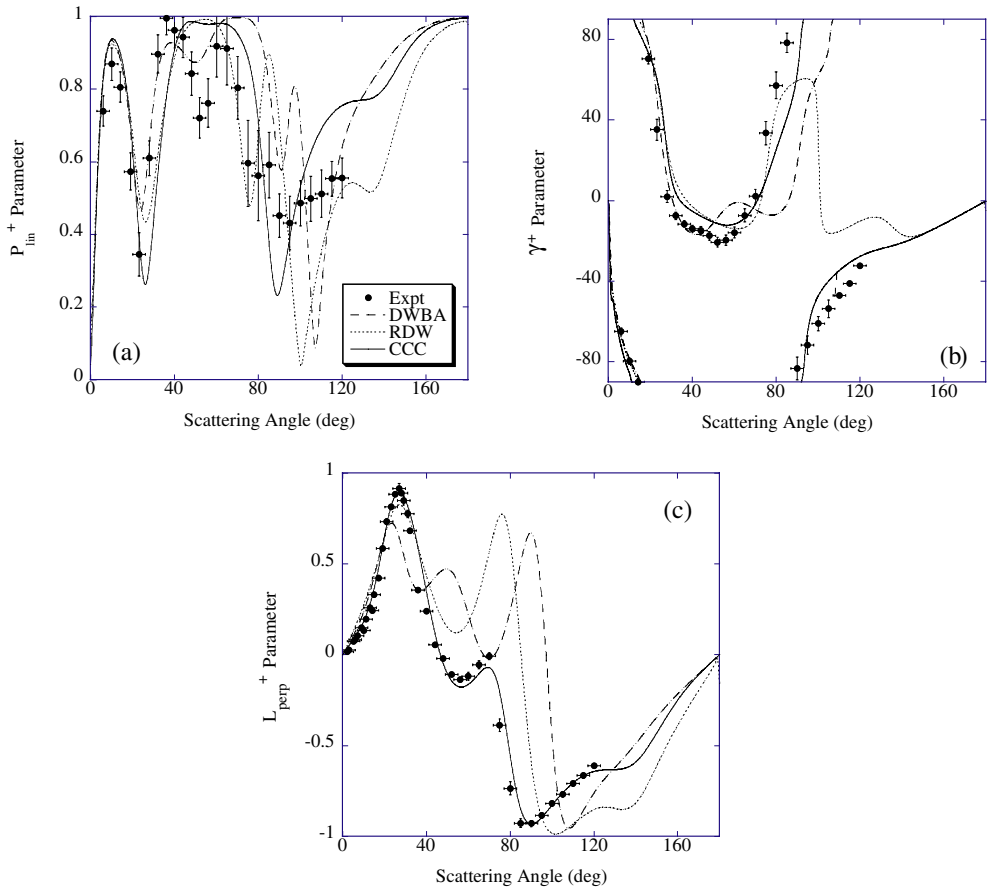

Figure 5. Measured values of the natural frame atomic collision parameters (a) $P^{+}_{\rm lin}$, (b) γ^{+} and (c) $L^{+}_{\perp}$ compared to the theoretical model calculations: CCC (solid line), DWBA (dashed line) and the RDW model (dotted line).

the CCC model agrees best for the remaining angles. The maximum predicted by the DWBA model at about 60° is not reflected in the data. The RDW and CCC models are in reasonably close agreement to 80°. For the P_3 Stokes parameter (figure 4(c)), excellent agreement with the measured data is achieved by the CCC model over all scattering angles. However, there is a tendency for the experimental data and the CCC curve to be displaced by about 5° at the higher scattering angles.

Given the lack of consistent overall agreement for the Stokes parameters between the experiment and theoretical models, it is not surprising that the experimental data for the derived parameter, $P_{\rm tot}$ is not reproduced by any of the models. The experimental data show several significant departures from the fully coherent value of unity while the theories predict two smaller excursions. Departure of the total polarization from unity is an indicator of the interference of the singlet and triplet channels and of the importance of exchange scattering in the collision process (Andersen *et al* 1988).

In a recent paper, Andersen and Bartschat (2002) presented theoretical calculations of Stokes parameters for caesium. Their theory employed a 40-state R-matrix with pseudo states (RMPS) model in which relativistic effects were included using a Breit–Pauli potential in the

Hamiltonian. These authors concluded that the contribution to the differential cross section and Stokes parameters by relativistic effects was negligible, and that it was doubtful that such effects could be measured in a superelastic scattering experiment using unpolarized electrons confirming the results of Karaganov *et al* (2002). The same conclusion might be expected to hold for the lighter rubidium target. This recent result further confirms the likelihood that ρ_{00} is zero.

The ACPs derived from the measured Stokes parameters using equations (4) are plotted in figure 5 where they are compared with calculations from the three theoretical models. As $P_{\rm lin}^{+}$ is derived from the magnitudes of P_1 and P_2, it is not surprising that its agreement with any of the theoretical models is poor. Only the CCC curve has as deep a first minimum while only the DWBA model predicts a minimum at 50°, although this minimum is not as deep as the measurements indicate. There is virtually no correlation between the measured values and the calculations for scattering angles greater than 90°. Conversely, the charge-cloud alignment angle, γ^{+}, which is related to the phase difference between P_1 and P_2, shows good agreement with the CCC calculation (figure 5(b)) over the entire measured angular range. There is no ambiguity for γ^{+}, and neither of the other models demonstrate the same level of agreement. This is also true for the transfer of angular momentum parameter, $L_{\perp}^{+}$. The disagreement noted above for P_3 holds for $L_{\perp}^{+}$ as these parameters are simply the inverse of each other.

5. Conclusions

In the work reported in this paper, the first measurement of Stokes parameters and atomic collision parameters for electron collision with rubidium are reported. The superelastic scattering method has been used to provide data at an electron impact energy of 20 eV. The data have been compared to calculation from three theoretical models of the collisional process.

Measurement of the parameter ρ_{00} indicates that *LS* coupling holds under the experimental conditions employed here, to within the experimental uncertainty. As none of the theoretical models considered here include relativistic effects in the interaction potential, it is valid to use these to model the collision process. None of the models accurately reproduce the experimental data. The CCC model performs best across all parameters but has areas of disagreement with the data. While no definitive evidence of the breakdown of *LS* coupling has been observed in these experiments, it is possible that relativistic contributions to the potential are still significant. Inclusion of a relativistic component in the theoretical models for rubidium would enable a more stringent comparison to be made.

The availability of electron spin-polarized data would greatly assist in the testing of such theories. To facilitate this aim, an experiment to investigate electron–rubidium collisions at 20 eV excitation energy employing spin polarized incident electrons has now commenced in the Griffith laboratory.

Acknowledgments

We would like to thank the Australian Research Council for providing funding for this work, and for providing a research scholarship for BH. IB acknowledges the support of the ARC and the Merit Allocation Scheme of the National Facility of the Australian Partnership for Advanced Computing.

References

Andersen N and Bartschat K 1996 *Adv. At. Mol. Phys.* **36** 1
Andersen N and Bartschat K 2002 *J. Phys. B: At. Mol. Opt. Phys.* **35** 4507
Andersen N, Bartschat K, Broad J T and Hertel I V 1997 *Phys. Rep.* **279** 251
Andersen N, Gallagher J W and Hertel I V 1988 *Phys. Rep.* **165** 1
Bray I 1994 *Phys. Rev.* A **49** 1066
Farrell P M, MacGillivray W R and Standage M C 1991 *Phys. Rev.* A **44** 1828
Farrell P M, Webb C J, MacGillivray W R and Standage M C 1989 *J. Phys. B: At. Mol. Opt. Phys.* **22** L527
Fischer A and Hertel I V 1982 *Z. Phys.* A **304** 103
Hall B V 1998 *PhD Thesis* Griffith University unpublished
Hall B V, Shurgalin M, Murray A J, MacGillivray W R and Standage M C 1999 *Aust. J. Phys.* **52** 515
Hanne G F 1983 *Phys. Rep.* **95** 95
Hermann H W, Hertel I V, Reiland W, Stamatovic A and Stoll W 1977 *J. Phys. B: At. Mol. Opt. Phys.* **10** 251
Hertel I V and Stoll W 1974 *J. Phys. B: At. Mol. Phys.* **7** 570
Karaganov V, Bray I, Teubner P J O and Farrell P 1996 *Phys. Rev.* A **54** R9
Karaganov V, Teubner P J O and Brunger M 2002 *Correlations, Polarization, and Ionization in Atomic Systems* ed D H Madison and M Schultz (New York: American Institute of Physics) p 196
Law M R and Teubner P J O 1995 *J. Phys. B: At. Mol. Opt. Phys.* **28** 2257
Li Y and Zetner P W 1994 *Phys. Rev.* A **49** 950
Murray A J, Turton B C H and Read F H 1992a *Rev. Sci. Instrum.* **63** 3346
Murray A J, Woolf M B J and Read F H 1992b *J. Phys. B: At. Mol. Opt. Phys.* **25** 3021
Registar D F, Trajmar S, Jensen S W and Poe R T 1978 *Phys. Rev. Lett.* **41** 749
Sang R T, Farrell P M, Madison D H, MacGillivray W R and Standage M C 1994 *J. Phys. B: At. Mol. Opt. Phys.* **27** 1187
Scholten R E, Shen G F and Teubner P J O 1993 *J. Phys. B: At. Mol. Opt. Phys.* **26** 987
Stockman K A, Karaganov V, Bray I and Teubner P J O 1998 *J. Phys. B: At. Mol. Opt. Phys.* **31** L867
Varcoe B T H, Hall B V, Johnson G, Johnson P, MacGillivray W R and Standage M C 2000 *Meas. Sci. Technol.* **11** N111
Zeman V, McEachran R P and Stauffer A D 1998 *Eur. Phys. J.* D **1** 117
Zetner P W, Trajmar S and Csanak G 1990 *Phys. Rev.* A **41** 5980